

Quasi-Static Transmission Error Behavior Under the Composite Effect of Temperature and Load

Aitor Arana, Jon Larrañaga, Ibai Ulacia, Mikel Izquierdo, & Miren Larrañaga

Introduction

Technological trends in automotive and aeronautical industries are pushing geared powertrains towards high rotational speeds with pitch line velocities approximating 100 m/s (Ref. 1), large gear ratios with low number of stages (Ref. 2) and minimum oil immersion depths (Ref. 3). At such conditions, thermo-mechanical issues are expected as bearings and gears are close to their thermal capacities.

Field experience in the turbomachinery industry has long proved that high-speed gearing is prone to thermal distortion effects. However, much of the knowledge remains restricted to the field of application and it is not available in the open literature. Seminal experimental work by Welch and Boron (Ref. 4) showed that in helical gear drives with relatively large face widths, the temperature of the teeth rises non-uniformly across the face width due to axial oil pumping. Longitudinal thermal gradients result in an uneven load distribution along the tooth trace and the authors pointed out that this behavior could be regenerative until tooth failure occurs. Subsequent works by Martinaglia (Ref. 5), Akazawa (Ref. 6), Matsumoto et al. (Ref. 7) and Amendola et al. (Ref. 8) prove such behavior and even numerically correlate thermal gradients to tooth root stress increase (Ref. 9).

Meanwhile, the number of evidences in small size gears is scarce and it is mostly concentrated on plastic gearing because thermal expansion coefficients are large and mechanical properties are temperature dependent. Wang (Ref. 10) concluded by finite element analysis of Nylon PA6 gears that because of temperature increase, the length of the contact path is expanded

with increased premature contact effects and multiple teeth in mesh. Later, Kashyap et al. (Ref. 11) experimentally analyzed the thermal expansion of Acetal spur gears and found that geometry change is mainly due to local pressure angle deviations that affect peak-to-peak transmission error at elevated temperatures. Even though references on thermally induced geometry distortion of steel gears are rare, recently, Hensel et al. (Ref. 12) have numerically shown that temperature increase can affect transmission error harmonic behavior when design contact ratios are close to an integer value. In the same direction, an experimental study by Luo and Li (Ref. 13) points out that temperature affects vibration amplitude of the system through thermally induced profile deviations, with temperature increases yielding larger vibration amplitudes.

In view of the lack of information on thermal distortion effects in small size steel gears, an experimental study of quasi-static transmission error behavior under thermomechanical conditions is carried out in this work. Composite effect of temperature and load on backlash, mean level of transmission error and its peak-to-peak value are experimentally studied and results are compared to analytical predictions.

Methodology

In order to analyze the thermo-mechanical behavior of external cylindrical gears, a specific back-to-back test rig has been built based on the standard FZG machine architecture (Ref. 14). The main differences between the designed test bench and those available in the market are the speed and torque limitations, which have been overcome to study high power density

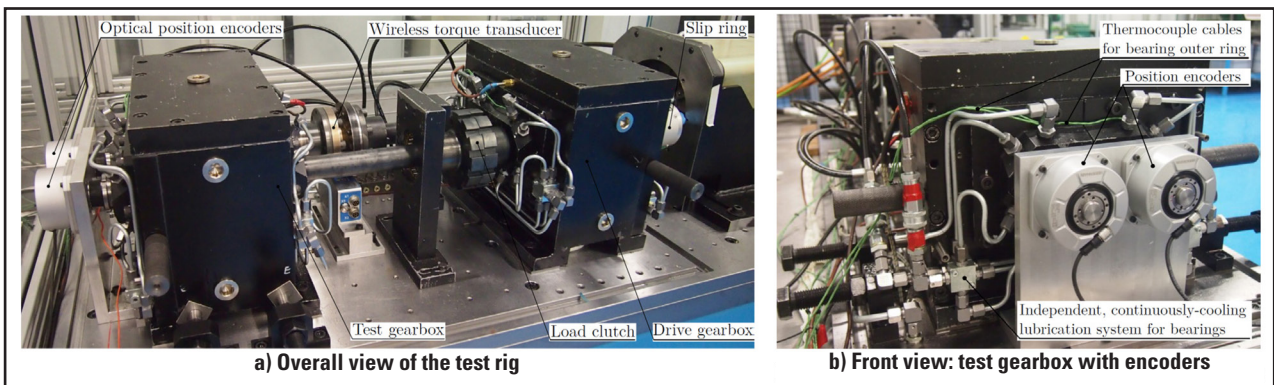


Figure 1 Designed test rig for gear thermomechanical behavior analysis.

transmissions. Furthermore, test and drive gear sets have been thermally isolated from their bearings, so that the thermal behavior of the gear pair can be studied independently from that of the bearings.

Test rig description. The designed test rig is shown (Fig. 1). It is composed of two equal gearboxes with inverse gear ratios (known as “test” and “drive”) following standard back-to-back configuration. Gearboxes are connected by two shafts; one of them being split in two parts with a load clutch in between for manual torque application with a lever arm. The traction motor rotates the main shaft so that the torque necessary to rotate the system is equal to the torque loss inside the loop. Two wireless, dual-range torque transducers located inside and outside the mechanical loop, measure the applied load and torque loss respectively.

In order to reach high circumferential speeds a liquid-cooled squirrel-cage induction AC motor for electric vehicles (EV) has been selected, reaching a maximum rotational speed of 10.000 rpm. Built-in sensors and position encoders allow accurate speed and torque control in the whole range. Moreover, in order to maximize tangential speeds, center distance has been increased up to 110 mm, so that the maximum attainable tangential velocity is 60 m/s, as larger diameters and gear ratios are allowed with respect to the standard FZG machine. Shafts and bearings have also been adapted and the maximum torque inside the loop now reaches 1000 Nm, which results in 1 MW maximum recirculating power.

When the test rig is subject to high speeds, considerable heating of the bearings arises which affects temperature distribution of the gear pair due to their proximity. To solve this issue, an independent lubrication circuit has been designed such that the oil from the bearings is physically separated from the gear oil sump by means of a specially designed housing. An ISO VG 46 oil is continuously pumped into each bearing housing through the lubrication pipes in Figure 1b at a minimum oil flow rate of 1 l/min. In order to avoid overflowing them, an additional suction pump has been installed which is driven by a servomotor and balances the oil level inside each housing by controlling the oil level in the tank with a digital level and a programmable logic controller (PLC). Meanwhile, gears inside the gearbox may be jet or dip-lubricated, and even oil-out conditions can be simulated without affecting bearing supports. In case of oil bath lubrication, the relative immersion depth is adjusted easily, and if necessary, oil is heated by means of high-power density thermoelectric resistances located inside a sealed aluminum plate submerged in the oil sump. A thermocouple immersed in the oil sump measures the temperature of the lubricant which is then heated by means of thermal resistances connected to a PID temperature controller.

The test rig includes several sensors to measure temperature, torque, speed, transmission error and oil condition. T-type thermocouples measure the temperature of different parts (bearings, housing, etc.) and a common data acquisition chassis

	Symbol	Set A	Set B
Normal module	m_n [mm]	3	
Normal pressure angle	α_n [°]	20	
Number of teeth	$z_{1,2}$ [-]	37, 37	25, 50
Profile shift coefficient	$x_{1,2}$ [-]	-0.1608, -0.1608	-0.0234, -0.7337
Face width	b [mm]	25	
Tip rounding	h_k [mm]	0.6	
Tolerance field acc. DIN 3967	E_s [-]	cd25	
Quality acc. ISO 1328	Q [-]	5	
Reference tool acc. ISO 53	[-]	A (1.25/1.00/0.38)	
Material and treatment	[-]	17NiCrMo6, case-hardened	

	Symbol	Value
Input speed	N_i [rpm]	60
Input torque	T_i [Nm]	50, 100, 200, 400, 600
Immersion depth	H/R [-]	0.5
Oil temperature	ϕ_o [°C]	50, 75, 100, 125, 150

synchronizes all signals. Temperatures of pinion and gear at several radial locations are measured and the rotating thermocouple signals are transmitted by means of a pair of slip rings. Moreover, each gearbox includes an oil condition sensor monitoring not only sump temperature, but water contamination and debris concentration as well — allowing for failure detection.

Finally, transmission error is measured with a pair of high-resolution optical angle encoders with $\pm 2.5''$ accuracy, equivalent to $\pm 0.6 \mu\text{m}$ for a 100 mm base diameter gear.

Test specimens. In this work, two spur gear sets are analyzed. Both are characterized by having a common 3 mm module, 25 mm face width and 20° pressure angle; while gear ratios are different: test set A is a 1:1 transmission while set B is 2:1. Additional information can be found in Table 1.

Note that the number of teeth is non-hunting and therefore each tooth will contact the same mate in the gear every time so that the composite manufacturing pitch and profile deviations will be constant for each mesh cycle. This allows to clearly identify thermal distortion effects; as variable composite tooth errors are not expected. Finally, both geometries have been manufactured with the same reference profile, material, quality and tooth thickness tolerance; the only difference being the profile shift coefficient which has been selected to balance specific sliding on each gear set. As a consequence, pinion and gear teeth geometry in set A are identical and those of set B are different due to dissimilar addendum modifications.

Operating conditions. The test program considers two steps: mechanical tests are carried out first and thermomechanical behavior is analyzed next. The former is used as a reference to analyze the effects of temperature increase on quasi-static transmission error. Table 2 summarizes working conditions for both sets.

Tests will be completed at 1 Hz constant rotational speed, which is considered sufficiently low to avoid introducing dynamic effects. Nevertheless, in order to guarantee quasi-static behavior, a preliminary dynamic study has been carried out and TE repeatability measurements have been completed. Besides, torque levels have been selected such that low and high unit loads are considered in combination with thermal effects. Nominal torque is 200 Nm and a total amount of five torque

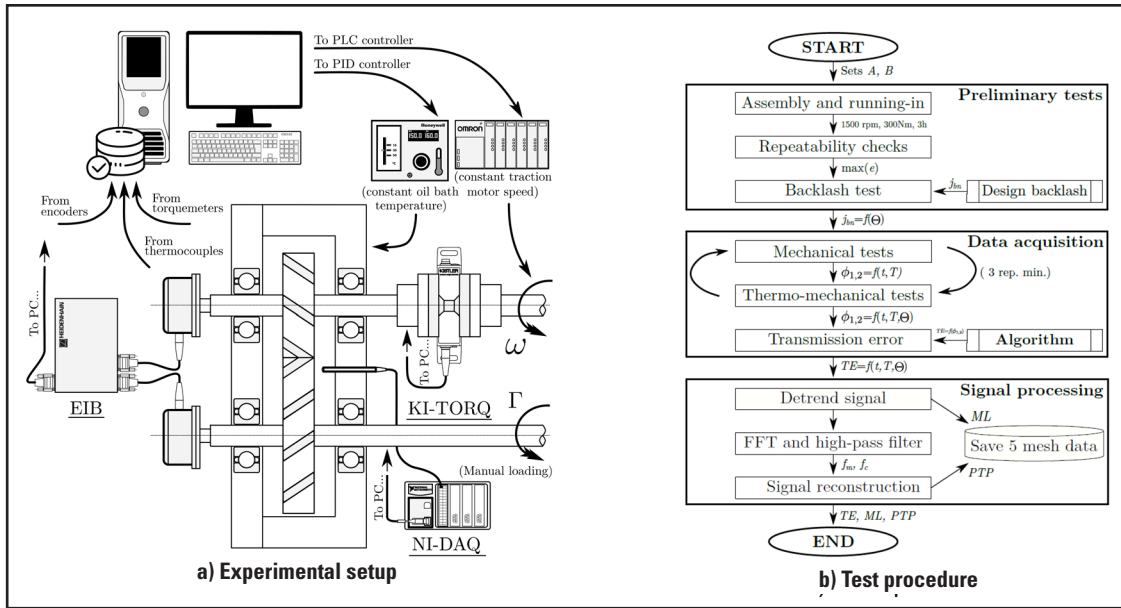


Figure 2 Experimental setup and procedure for thermo-mechanical quasi-static TE measurement.

levels is considered.

Finally, thermo-mechanical tests are completed by progressively heating the oil sump up to 150°C while rotating the gear pair at constant speed and prescribed torque, until the steady-state temperature is reached. A paraffinic mineral oil ISO VG 100 (Ref. 15) is used in the tests and the relative immersion depth is kept constant, just below the gear hub to ensure that radial temperature gradients are negligible.

Experimental procedure. The experimental setup and test procedure for the thermo-mechanical tests are graphically summarized in Figures 2a and 2b respectively. First, gears are mounted on the test and drive gearboxes and contact pattern is checked. If both gears are correctly assembled, lubricating oil is poured into the sump until the desired immersion depth is reached and torque level is adjusted with the lever arm. Once the exact value of torque is measured in the loop's torque transducer, bolts are tightened in the load clutch and the lever arm is removed. Then, motor speed is preset in the control software and prescribed value is sent to the PLC controller which turns on the traction motor. Simultaneously, the bearing-independent lubrication pumps are turned on along with the motor cooling system. Gears are run-in for at least three hours at 1,500 rpm and 300 Nm torque. Afterwards, encoders are mounted on the input and output shafts of the test gearbox and both are connected to the evaluation unit. Finally, gear thermocouples and slip ring are mounted on the drive gearbox which is connected to the data acquisition chassis. Both gearboxes being identical, temperature measurements in the drive gearbox can be extrapolated to test one.

Mechanical tests are carried out first at room temperature (20 ±1°C). Torque is preset to the first load stage of the test program and motor is rotated at constant 60 rpm rotational speed. Then, angular position measurements are conducted at steady-state rotational speed comprising a minimum of 20 full rotations. Then, the motor is stopped and next load stage is prescribed with the lever arm. The measurement procedure is repeated with each of the torque levels until the maximum load

is reached. Once the first load cycle is finished, the next cycle begins and the same steps are repeated from the lowest load stage to the highest one. A minimum of three repetitions are carried out in mechanical tests, each of them comprising several torque levels. Although no significant temperature increase is expected in these tests due to their short duration, component temperatures are monitored to ensure thermal effects are minimal.

The test program continues with the thermo-mechanical tests. The general procedure is kept but this time oil sump temperature is increased progressively in each load stage. Once torque value is preset, traction motor is rotated at constant speed and oil sump is heated with thermal resistances. Oil temperature is measured with a thermocouple immersed in the oil sump which sends instantaneous values to the PID controller and the acquisition system. The temperature of the oil bath, gear and housing is monitored and when steady-state condition is reached, angular position measurements are conducted following the procedure of the mechanical tests. Temperature is increased afterwards and when the next steady-state thermal stage is reached, measurements are completed in the same way. When the maximum temperature level for the considered load stage is attained, measurements are stopped until the whole system is cooled down. Then, next load stage is prescribed and the process is repeated. When all load-temperature combinations are finished, the process starts again until three full repetitions are completed.

Finally, when all tests in set A are finished, set B is tested following the same procedure. In between, additional tests such as no-load transmission error tests and backlash measurements are performed.

TE measurement. Transmission error (TE) is defined as the variation of the output rotational motion of the driven gear for constant rotational speed in the driver one due to elastic effects and clearances in the mesh. Therefore, TE is a relative magnitude relating angular positions of pinion and gear, which can be measured by the optical encoders. In terms of the length of the

line of action, TE can be computed following Equation 1 and the order of magnitude of its fluctuation at a specific torque is several microns for common gear sets.

$$TE = r_{b2} \cdot \Delta\theta_2 - r_{b1} \cdot \Delta\theta_1 \quad (1)$$

where r_{b1} and r_{b2} are the base diameters of pinion and gear respectively and $\Delta\theta_1$ and $\Delta\theta_2$ are the (1)

incremental angular positions relative to the starting position of the measurement. From Equation 1 one realizes that TE is always a negative parameter as the driven gear lags behind its theoretical conjugate position due to elastic deflections and backlash.

When transmission error is directly computed following Equation 1 the resulting curve presents a sinusoidal shape (Fig. 3a), characterized by a low frequency amplitude related to gear eccentricity and assembly errors and a high frequency cyclic variation due to time varying stiffness of the meshing teeth (Fig. 3d). In this work, thermomechanical effects are analyzed in the high frequency term which is related to tooth geometry and backlash. The influence of gear eccentricity is filtered out while maintaining the shape of the cyclic variation at mesh frequency with characteristic mean levels and peak to peak values. To this aim, a Fast Fourier Transform (FFT) is carried out followed by a high-pass filtering of the signal as shown (Fig. 3).

First, the original signal is detrended by an amount equal to the mean level of the initial measurement, so that the sinusoidal

curve is located on the abscissa as in Figure 3a. If the FFT is performed with the original signal, a big amplitude arises at 0 Hz masking small amplitudes of interest; hence the offset must be removed beforehand. However, the mean value of TE is preserved for signal reconstruction as it depends on the initial position of the gear pair, the applied load, temperature and available backlash.

Then, Fast Fourier Transform is computed in Figure 3b. Mesh frequency f_m in these tests corresponds to the number of teeth z as the shaft rotation frequency is 1Hz. Subsequent harmonics are located and N integer times the mesh frequency. Gear eccentricities to be filtered out are long-term errors (below mesh frequency) therefore, the high-pass filter must keep frequencies above the cut-off value f_c (in these tests $f_c \cong \frac{1}{2} \cdot f_m$). Once the original signal has been filtered, it can be reconstructed by computing the inverse transform (see Figure 3c) and finally, a set of 5 mesh cycles is selected for analysis, mean peak-to-peak transmission error is measured and initial offset is added to keep the mean level as shown (Fig. 3d).

Results

In the following section experimental results are summarized. Three types of measurements are shown: i) unloaded backlash tests at different temperatures, ii) loaded TE tests at room temperature and iii) full thermo-mechanical tests. In all cases, mean level of TE and peak-to-peak values are analyzed.

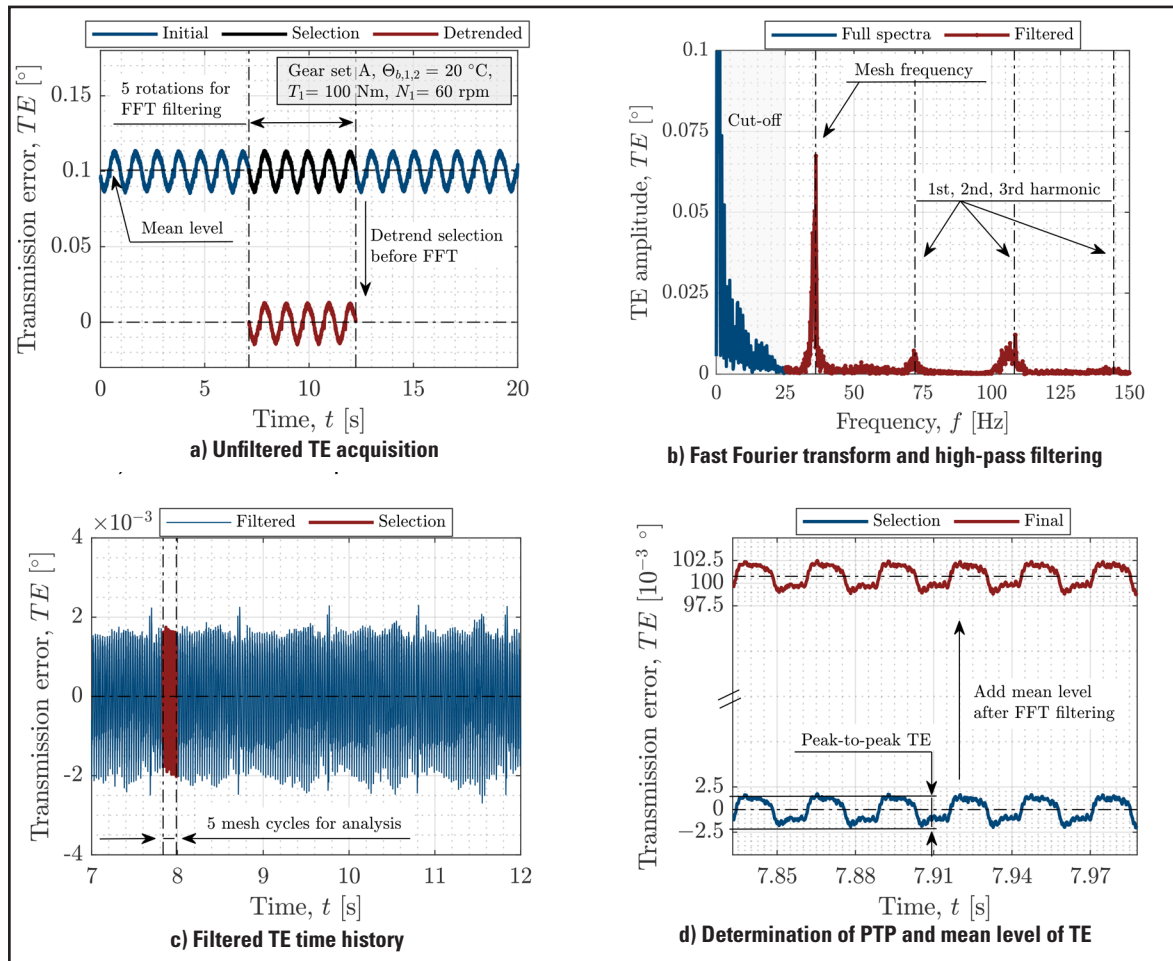


Figure 3 Sample TE measurement procedure in gear set A at 60 rpm and 100 Nm torque.

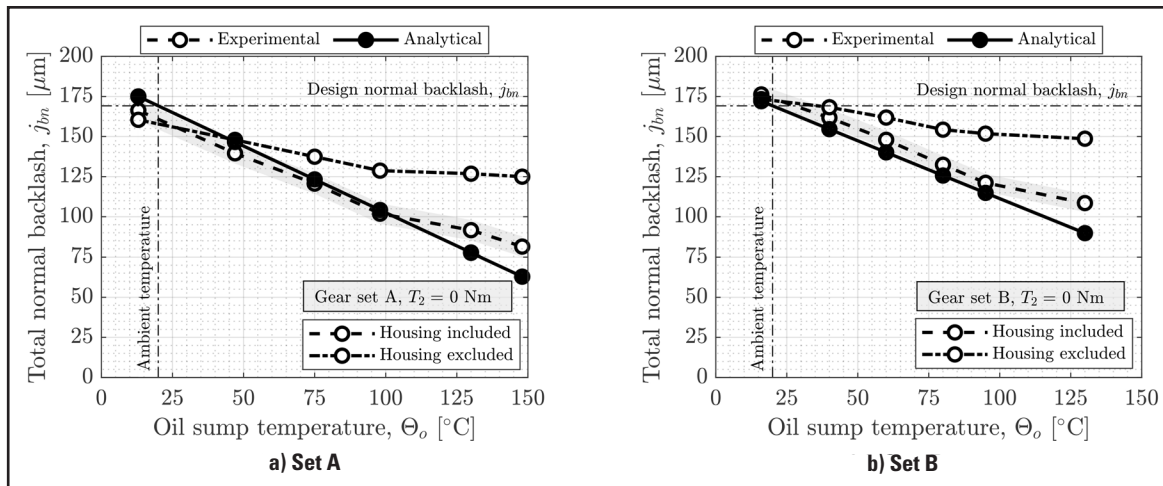


Figure 4 Temperature effect on total normal backlash reduction.

Backlash tests. Backlash tests are preliminary measurements to characterize the amount of available clearance at increasing oil sump temperatures. These tests are carried out before thermomechanical ones and they are used to validate the influence of temperature on backlash so that a correlation between this parameter and the mean level behavior can be established in future experiments. The driven gear position is fixed with the load clutch support while the pinion is rotated in clockwise and counter-clockwise directions until contact of the flanks occurs and loop torque signal is increased in the torque transducer. Several repetitions are completed in three different angular positions and constant oil sump temperature. The graphical representation of the measurements of both encoders shows the amount of available backlash and the mean value of the different measurements is used for comparison with the design backlash. Figure 4 depicts the influence of temperature on total normal backlash, j_{bn} , relative to the design value. Analytical predictions meet the design value at ambient temperature while increasing the oil temperature reduces the amount of available backlash linearly; which is the expected behavior if pinion and gear temperatures are assumed to be constant and equal to that of the oil sump. Meanwhile, experimental measurements follow the analytical prediction provided that the influence of the housing expansion is suppressed as shown by DIN 3967 standard (Ref. 16). Note that gear dilatation tends to reduce backlash while center distance expansion increases it. Hence, if the effect of the latter is not suppressed from the raw experimental measurement, it is not possible to analyze the influence of the gear expansion term.

Both gear sets show the same trend with temperature with analytical predictions following closely at least up to 100°C temperature. However, it is to be noted that the experimental

measurement slightly deviates from the analytical predictions due to several reasons. On the one hand, housing and gear manufacturing and assembly tolerances affect this correlation and on the other hand, theoretical linear thermal expansion coefficient for steel may deviate up to $\pm 5 \cdot 10^{-7} \text{ K}^{-1}$ from its real value. Moreover, temperature differences may exist between the preset oil sump temperature and that of pinion and gear. Although manufacturing tolerances of the housing and thermal expansion coefficient deviations have been considered in the shaded error bar, the temperature differences are difficult to control, as it will be shown later in the discussion, especially at the highest temperatures where the largest deviations arise.

Loaded TE tests. Figure 5 summarizes loaded transmission error measurements for both gear sets. Analytical predictions according to the thin slice model presented in (Ref. 17) have been included to highlight the expected behavior.

If attention is paid to the TE diagrams in Figs. 5a and 5b, it is observed that load tends to increase both, transmission error mean level and peak-to-peak values; therefore, the gear is increasingly delayed with respect to its theoretical position. Reference position corresponding to half normal backlash and coincident with the no-load transmission error term is highlighted in all diagrams such that increasing separation from this position indicates that the backlash gap increases with load. Moreover, it is also remarked that peak-to-peak values increase with torque while the premature contact effect tends to contract the region of single tooth contact at higher loads. This behavior is consistent with scientific literature and it is also predicted by the analytical model.

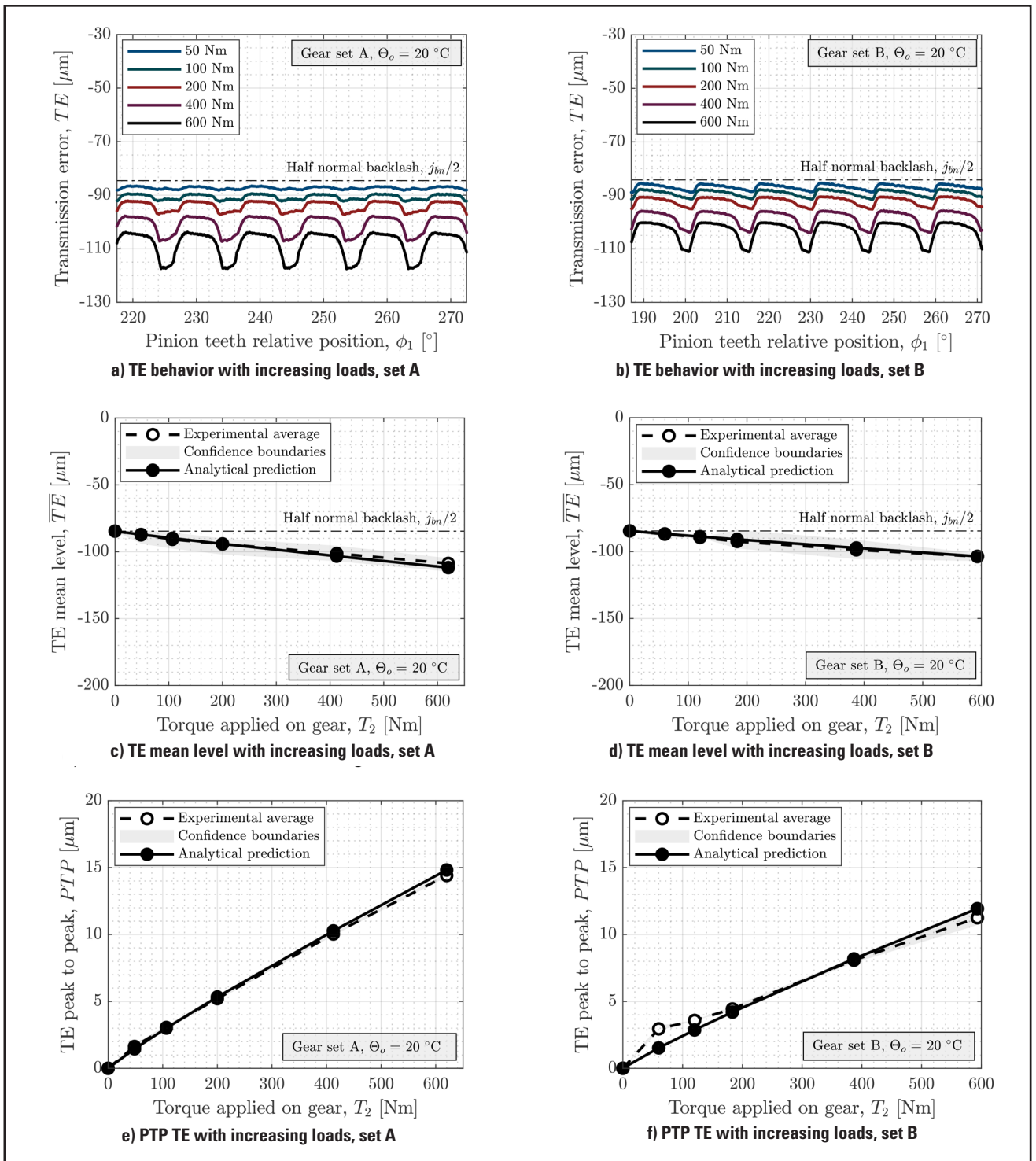


Figure 5 Experimental loaded TE measurements for gear sets A and B at 20°C temperature.

Loaded and thermally affected TE tests. Figure 6 shows the influence of increasing temperature at constant torque. The initial TE curve at ambient temperature is shifted because the backlash gap is reduced while the overall shape of TE remains unchanged. No apparent peak-to-peak variation is noticed at first sight and no premature contact effect is clearly visible from subfigures 6a and 6b. If the latter are compared to the loaded results, it is observed that the effect of temperature on mean level is greater than that of load which is confirmed by the slope

of the curve in subfigures 6c and 6d. Moreover, if the mean level behavior in these figures is compared to that of backlash in Figure 4 it is confirmed that the shift in mean level correlates to backlash change. Besides, it is interesting to remark that if pinion and gear temperatures are constant and equal to that of the oil sump, the analytical trend does not predict any significant change in peak-to-peak TE behavior. However, experimental results in subfigures 6e and 6f show increasing peak-to-peak values with temperature.

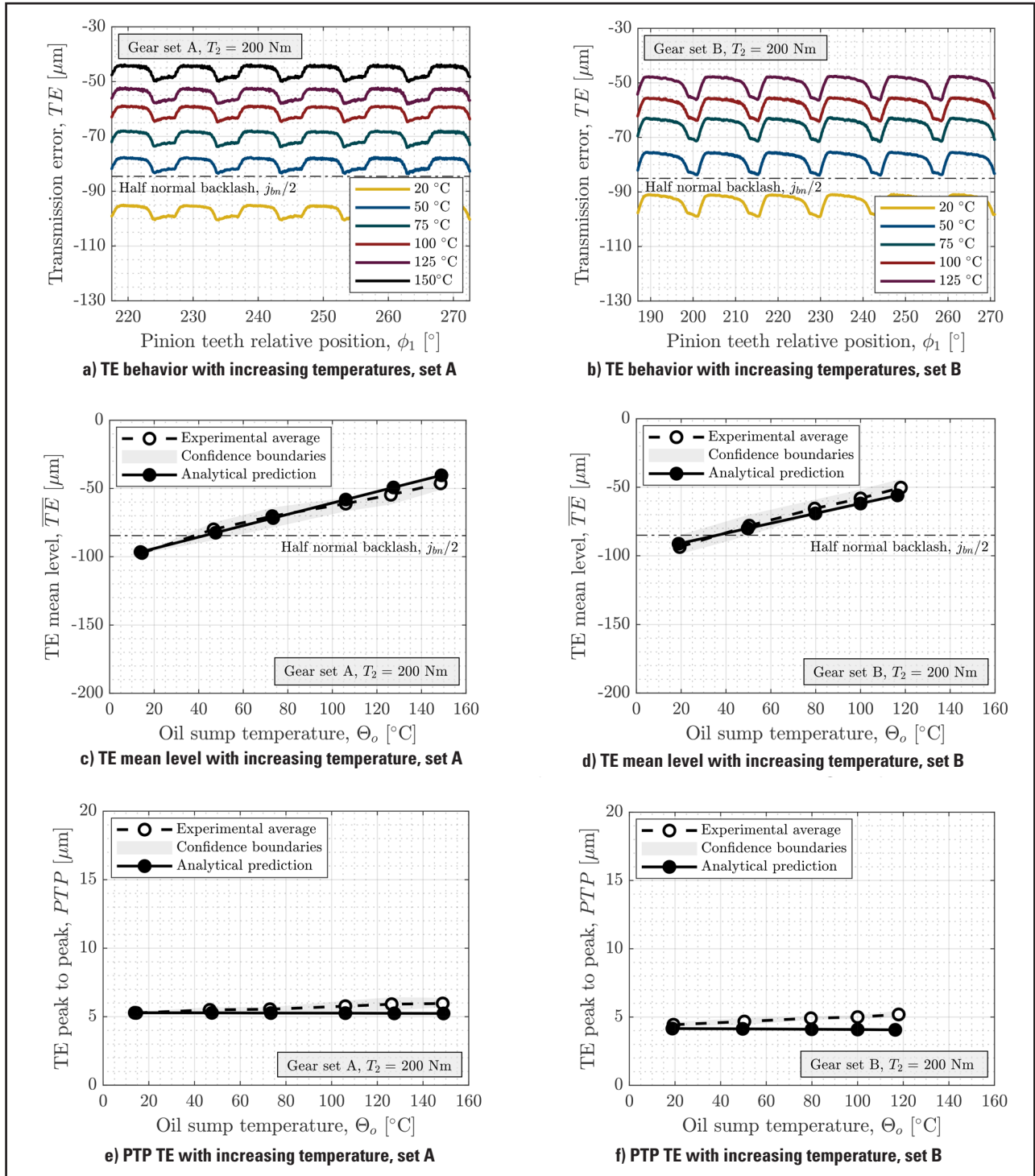


Figure 6 Experimental thermal TE results for gear sets A and B at 200 Nm torque.

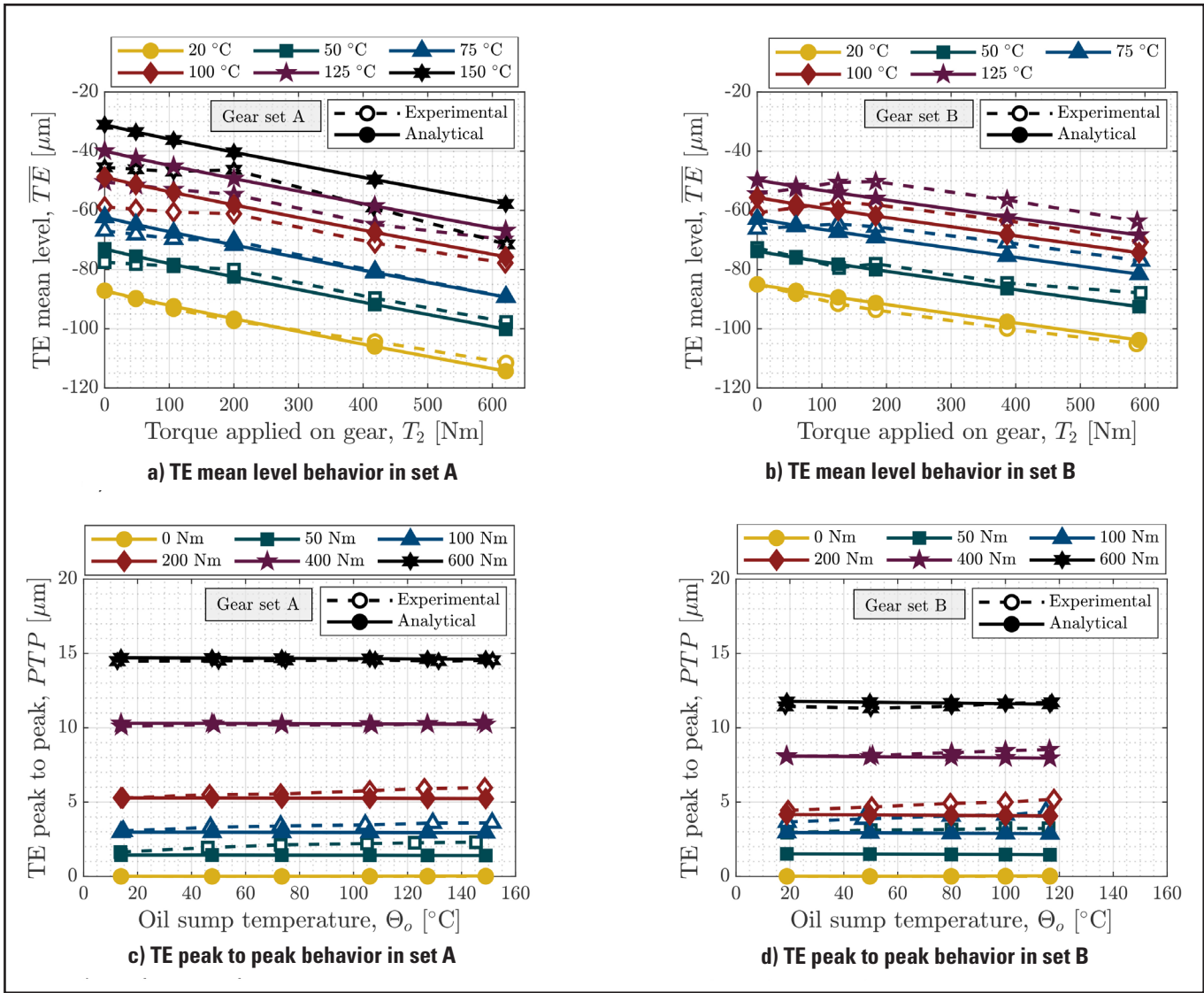


Figure 7 Experimental and analytical TE mean level and PTP comparison for variable temperatures and torques in both gear sets.

Summary of Experimental Results

Finally, Figure 7 gathers all thermomechanical results in gear sets A and B. All torque and temperature combinations repeat the mean level and peak-to-peak patterns described in preceding figures. Increasing torque decreases TE mean level (stretches available backlash gap) while increasing temperature increases it (contracts available backlash gap); the influence of temperature on the latter being more prominent.

Meanwhile, peak-to-peak value is mostly influenced by torque and experimental results show that it slightly increases with temperature, which is not predicted by the analytical model where values remain almost constant. Furthermore, it is interesting to note that the effect of temperature on experimentally measured peak-to-peak seems to be more pronounced at low torque. Such differences specially arise at the highest temperatures and they may be explained by existing thermal gradients between components as shown later.

Discussion

Constant temperature increase. Figure 8 depicts the effect of diameter growth on spur gear teeth profile and mesh behavior. A radial expansion results in a pitch increase, local pressure angle deviation and normal backlash decrease.

If pinion and gear temperature increase are equal, $\Delta\theta_{b1} = \Delta\theta_{b2}$, no relative pitch deviation exists and profile inclination errors are equal in pinion and gear as predicted by Equations 2 and 3, respectively. Therefore, mesh behavior should not be affected by constant temperature increases and peak- to-peak TE is expected to be exclusively ruled by torque.

$$f_{pt} = p_{yt}' - p_{yt} = \tau(r_y' - r_y) 2 \cdot \pi z^{-1} u(r_y) = m_t \cdot \pi \cdot \alpha_L \cdot \Delta\theta_b \quad (2)$$

$$f_\alpha \approx -\Delta d_b \cdot [d_b \cdot \tan(\alpha_{yt})]^{-1} = -\alpha_L \cdot \Delta\theta_b [\tan(\alpha_{yt})]^{-1} \quad (3)$$

where m_t is the module, α_L is the linear thermal expansion coefficient and α_{yt} is the local pressure angle.

However, it can be analytically proved that a constant temperature increase does lead to a constant backlash reduction in the line of action and therefore TE curves are shifted as experimentally observed in Figures 6a and 6b. If Equation 1 is broken down in loaded and unloaded terms, we have:

$$TE = r_{b2} \cdot [\Delta\theta_{2,L} + \Delta\theta_{2,NL}] - r_{b1} \cdot [\Delta\theta_{1,L} + \Delta\theta_{1,NL}] = r_{b2} \cdot \Delta\theta_{2,L} - r_{b1} \cdot \Delta\theta_{1,L} + NLTE \quad (4)$$

where $NLTE$ is the no-load transmission error term representing composite geometry deviations, $\Delta\epsilon_1 + \Delta\epsilon_2$. Now, consider the following relation for profile thermal distortion in the base tangent plane:

$$\Delta\epsilon(\xi_y) \approx u(\xi_y) \cdot \sin(\alpha_{yt}) = [r_b \cdot \sqrt{1 + \xi_y^2} \cdot \Delta\theta_2 + \alpha_L] \cdot \sin[\arctan(\xi_y)] \quad (5)$$

where r_b is the base radius and ξ_y is the roll angle at any profile position. Applying the inverse trigonometric relation $\sin[\arctan(\xi_y)] = \xi_y (1 + \xi_y^2)^{-1/2}$, the preceding Equation 5 can be rewritten as:

$$\Delta\epsilon(\xi_y) \approx \Delta\theta_b \cdot \alpha_L \cdot r_b \cdot \xi_y = \alpha_L \cdot \Delta\theta_b \cdot \rho_y = \alpha_L \cdot \Delta\theta_b \overline{T_n P_y} \quad (6)$$

where $T_n P_y$ is the distance between any point in the profile and the tangent to the base circle. Equation 6 describes a linear

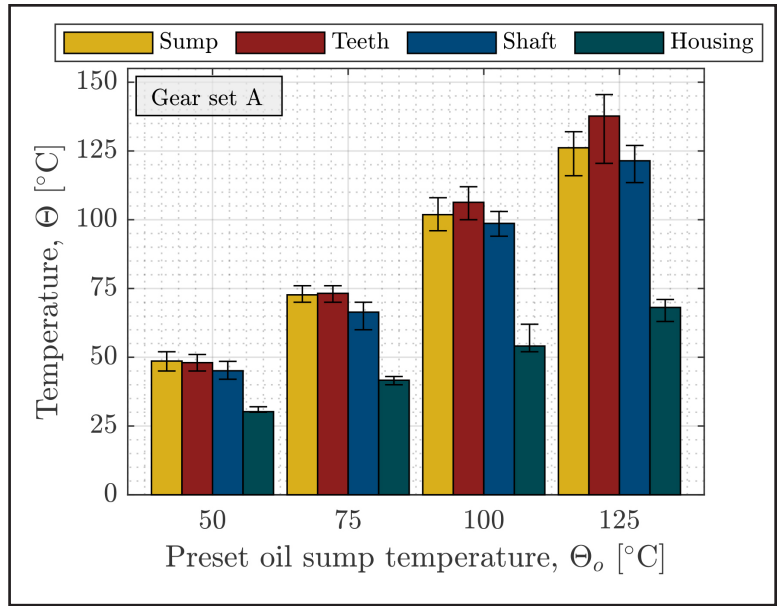


Figure 9 Gearbox temperature distribution relative to preset temperature in PID.

behavior of profile thermal distortion $\Delta\epsilon$ with roll angle ξ_y , which is consistent with Equation 3. Computing backlash decrease for equal pinion and gear temperatures we have:

$$\Delta j_{bn}' = \Delta j_{bn} - \Delta\epsilon_H = \Delta j_{bn} - [\alpha_w \cdot \alpha_{L,H} \cdot \Delta\theta_H \cdot \sin(\alpha_{wt})] \quad (7)$$

which is constant for gear pairs with the same material. This proves that under these conditions the $NLTE$ term in Equation 4 is constant as well and the TE diagram is shifted with respect to the purely loaded behavior. If housing expansion $\Delta\epsilon_H$ is considered together with Equation 7, the amount of total backlash change $\Delta j_{bn}'$ is reduced but maintains the constant trend along the line of action observed experimentally.

$$\Delta j_{bn}' = \Delta j_{bn} - \Delta\epsilon_H = \Delta j_{bn} - [\alpha_w \cdot \alpha_{L,H} \cdot \Delta\theta_H \cdot \sin(\alpha_{wt})] \quad (8)$$

Thermal gradients. Equations 4 to 8 prove that an equal temperature increase in pinion and gear does not affect the TE curve shape because relative profile deviations are constant. Only backlash (i.e. mean level of TE) is reduced. However, it has been observed that peak to peak TE slightly increases in almost

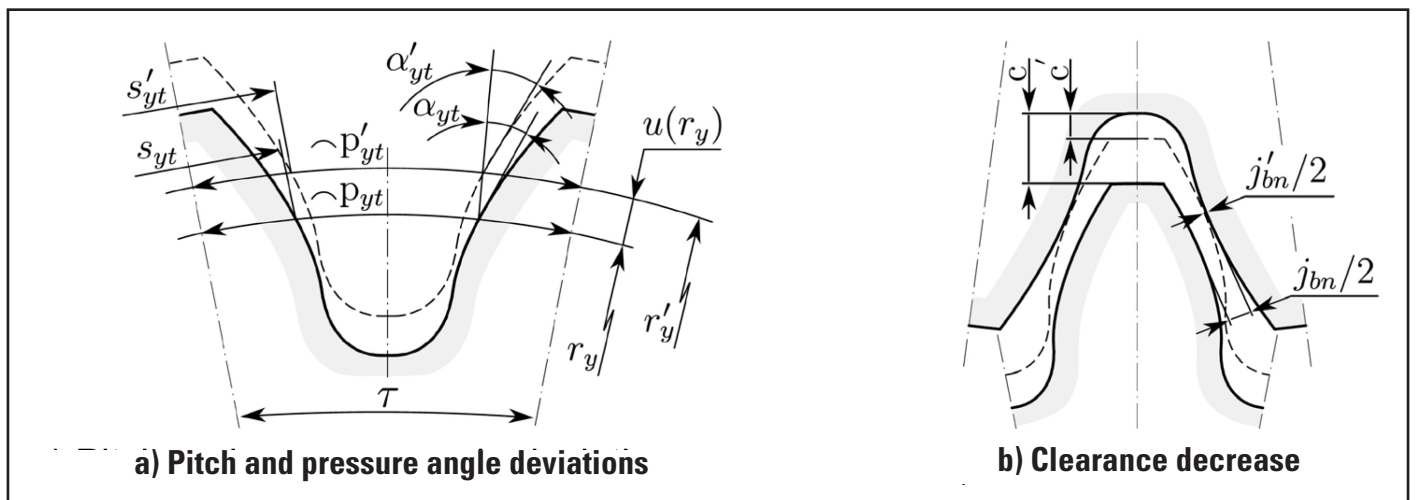


Figure 8 Effects of temperature increase on profile geometry and mesh behavior.

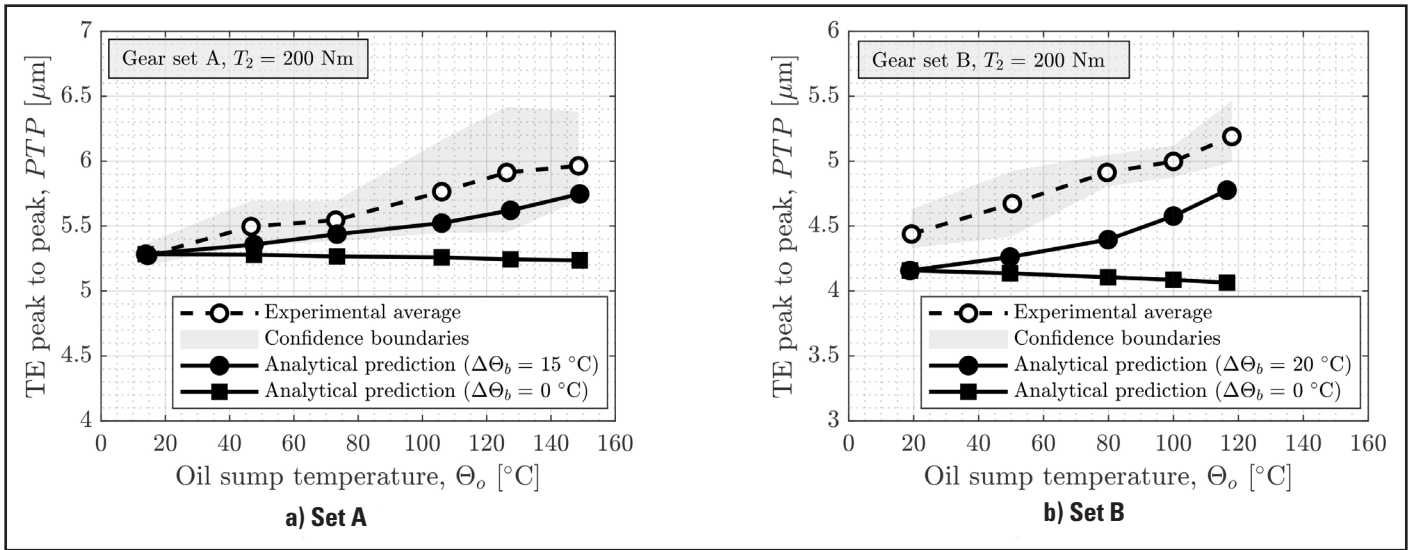



Figure 10 Influence of thermal gradient on peak-to-peak transmission error.

all test cases at the highest temperatures, which is not followed by analytical predictions.

Figure 9 summarizes measured mean temperatures and corresponding deviations of different parts of the gearbox for each temperature stage. At oil bath temperatures below 100°C, the steady state sump temperature is almost equal to the preset value and no significant temperature difference exists between the oil sump and the gear teeth. However, at higher temperatures, the standard deviation increases significantly indicating that the PID control hardly maintains oil sump temperature. Moreover, gear teeth temperature is higher than that of the oil bath, probably due to friction coefficient increase which progressively heats gear teeth above the oil bath temperature due to surface sliding.

In cases where the tooth temperature is higher than that of the oil, the available backlash should be reduced more than expected according to Equation 7. Therefore, experimentally measured mean level of transmission error in Figure 7a should overcome the predicted value, but this is not the case. It is to be noted in Figure 9 that at high temperatures not only thermal gradients arise between the oil sump and the gear teeth but also between the teeth and the shaft. Consequently, radial thermal gradients prevent maximum tooth deformations and corresponding backlash reduction. The final mean level depends on the exact temperature distribution for each case. Moreover, the existence of temperature differences between pinion and gear also explains the increasing peak-to-peak TE with temperature. Figure 10 shows the influence of thermal gradients between pinion and gear on both gear sets. As expected, peak-to-peak transmission error computed including temperature differences approaches the experimental result.

Conclusions

In this work an experimental study of thermo-mechanical quasi-static transmission error behavior has been developed. Scientific literature review presented in the introductory paragraphs has shown that no experimental evidence on the composite effect of temperature and torque on transmission error exists up to date. Then, a novel back-to-back test rig for high-speed gears has been described, experimental methodology has been presented and finally, measurement results have been summarized. Tests have been conducted at low rotational speed, constant torque and constant oil sump temperatures such that pinion and gear teeth temperature is assumed to be equal to that of the oil bath. Overall results show that the effect of temperature and torque coexist in TE diagrams. Both parameters have a significant role in the mean level of transmission error while the influence of torque on peak-to-peak is prominent relative to that of temperature. Furthermore, it has been shown that temperature increase reduces the amount of available backlash and therefore mean level of transmission error is affected. Both parameters have been shown to be correlated and an analytical proof has been provided. However, the analytical model has not predicted the experimentally observed variation of peak-to-peak TE with increasing temperature and discrepancies have been attributed to thermal gradients between components. 

References

1. Forschungsvereinigung Antriebstechnik. Speed4E projekt: Hyper-Hochdrehzahl für den elektrifizierten automobilen Antriebsstrang zur Erzielung maximaler Reichweiten. [Online]. Retrieved 18 September, 2018, from www.speed4e.de.
2. Gwinner, P., K. Stahl, S. Rupp and A. Strube. Innovative High-speed Powertrain Concept for Highly Efficient Electric Vehicles. *ATZ Worldwide* Vol. 119 (2017), pp. 66–71.
3. Neurouth, A., C. Changenet, F. Ville, M. Octrue and E. Tinguy. Experimental Investigations to Use Splash Lubrication for High-Speed Gears. *ASME Journal of Tribology*, Vol. 139:6 (2017).
4. Welch W.P. and J.F. Boron. Thermal Instability in High Speed Gearing. *Journal of the American Society for Naval Engineers*, Vol. 72:3 (1960), pp. 471–486.
5. L. Martinaglia. Thermal behavior of high-speed gears and tooth correction for such gears. *Mechanism and Machine Theory*, Vol. 8:3 (1973), pp. 293–303.
6. Akazawa, M., T. Tejima and T. Narita. Full Scale Test of High Speed, High Powered Gear Unit-Helical Gears of 25,000 PS at 200 m/s PLV. *Proceedings of the ASME International Power Transmissions and Gearing Conference*. 80-C2/DET-4. 1980.
7. Matsumoto, S., Y. Tozaki and M. Fukutomi. Temperature distribution in teeth and blanks of ultra high-speed gears, 1st report. *JSME International Journal, Series C: Mechanical Systems, Machine Elements and Manufacturing*, Vol. 44:1 (2001), pp. 203–209.
8. Amendola, J.B., J.B. Amendola III and D. Yatzook. Longitudinal Tooth Contact Pattern Shift. *Proceedings of the AGMA Fall Technical Meeting*. 11FTM18. 2011.
9. Tozaki, Y., S. Matsumoto and M. Fukutomi. Temperature distribution in teeth and blanks of ultra-high-speed gears, 2nd report. *JSME International Journal, Series C: Mechanical Systems, Machine Elements and Manufacturing*, Vol. 44:1 (2001), pp. 210–216.
10. J. Wang. Numerical and experimental analysis of spur gears in mesh. PhD thesis. Curtin University of Technology, 2003.
11. S. Kashyap et al. Methods of describing plastic gear geometry after a temperature change with application to the prediction of gear load distribution. *Proceedings of the ASME International Design Engineering Technical Conferences*. DETC2011-47501. Vol. 8 (2011), pp. 497–505.
12. E. Hensel et al. Thermal Influences on Gear Micro Geometry and Acoustic Excitation. *Romax Technology European User Forum*, 2015.
13. Luo B. and W. Li. Experimental study on thermal dynamic characteristics of gear transmission system. *Measurement*, Vol. 136 (2019), pp. 154–162.
14. *International Organization for Standardization*. ISO 14635-1: FZG test method A/8.3/90 for relative scuffing load-carrying capacity of oils. Technical standard, 2000.
15. E.M. Laukotka. Datensammlung Referenzzöle. Technical report 660. Forschungsvereinigung Antriebstechnik, 2007.
16. Deutsches Institut für Normung. DIN 3967: Backlash, Tooth Thickness Allowances, Tooth Thickness Tolerances. Technical standard., 1978.
17. Arana, A., A. Iñurritegui, J. Larrañaga and I. Ulacia. “Influence of thermal distortion on load distribution, transmission error and premature contact,” *Proceedings of the 2018 International Gear Conference*, Vol. 1, pp. 446–459.

For Related Articles Search

transmission error

at www.geartechnology.com

Dr. Ing. Aitor Arana Ph.D. is a lecturer and researcher in the Department of Mechanical and Industrial Production in Mondragon Unibertsitatea in Spain since 2008. He holds two mechanical engineering degrees from Ecole Centrale de Nantes in France and Mondragon Unibertsitatea in Spain, a Master of Research on Applied Mechanical Sciences and a Ph.D. thesis in thermo-mechanical behavior of gear transmissions. His main research expertise is in the field of mechanical design, tribology and analytical modelling of machine element behavior (gears, bearings, spline couplings, ball-screws..) regarding performance, durability and/or NVH. He has participated in 17 research projects funded by industry and public administrations and he has published 5 journal papers, 1 patent and 19 conference contributions.



Dr. Ing. Jon Larrañaga Ph.D. is a lecturer and researcher in the Department of Mechanical and Industrial Production in Mondragon Unibertsitatea since 2011. His main research expertise is in the field of mechanical design, simulation and experimental validation of mechanical components (gears, bearings, spline couplings, ball-screws..) regarding performance, durability and/or NVH. During his Ph.D. He was visiting research scholar at the Fachschule Rosenheim (Germany) and a postdoctoral research stay at the Institute for Technology Research and Innovation of the Deakin University (Australia). He has supervised 2 Ph.D. thesis (currently supervising 4 Ph.D. students), more than 30 bachelor and master thesis. He has published one book chapter, 12 journal papers, 3 patents and more than 40 conference contributions. He has participated in more than 30 research projects funded from both industry and public administrations.



Dr. Ing. Ibai Ulacia Ph.D. is the Head of research group Structural Mechanics and Design (DME) research in the Department of Mechanical and Industrial Production in Mondragon Unibertsitatea. He is accredited as “Profesor Doctor de Universidad Privada” since 2015 and holds two accredited research periods (a.k.a. sexenio de investigación): 2007-2012 and 2012-2018. He has supervised 9 Ph.D. thesis and more than 40 bachelor and master thesis. He has published 2 book chapters, 31 journal papers (cited more than 800 times), 2 patents and more than 70 conference contributions (4 keynote or invited talks). He has participated in more than 50 research projects funded from both industry and public administrations.



Dr. Ing. Mikel Izquierdo Ph.D. is a lecturer and researcher in the Department of Mechanical and Industrial Production in Mondragon Unibertsitatea since 2018. He received his Bachelor's Degree in Mechanical Engineering, Master's Degree in Industrial Engineering and Ph.D. in the automotive suspension field from Mondragon Unibertsitatea in Spain. He is currently a researcher of the Structural Mechanics and Design (DME) research group. His research interests are oriented to modelling, prototype development and experimental characterisation of machine elements and mechanisms.



Dr. Ing. Miren Larrañaga Ph.D. is a lecturer and researcher in the Mechanical and Industrial Production Department of Mondragon Unibertsitatea. She has been a researcher in the Structural Mechanics and Design research team since 2015, mainly focused on the topics of fatigue characterization and residual stress management.

